

1 **Have Tropical Cyclones Been Feeding More**
2 **Extreme Rainfall?**

3
4 **K.-M. Lau¹, Y. P. Zhou², H.-T. Wu³**

5 ¹ Laboratory for Atmospheres, NASA, Goddard Space Flight Center, Greenbelt, MD.
6

7 ² Goddard Earth Sciences & Technology Center, University of Maryland Baltimore
8 County, Catonsville, MD

9 ³ Science Systems and Applications, Inc., Lanham, MD.
10
11
12
13
14

15 Journal of Geophysical Research
16
17

18 Revised September 2008

1 **Abstract**

2 We have conducted a study of the relationship between tropical cyclone (TC) and
3 extreme rain events using GPCP and TRMM rainfall data, and storm track data for July
4 through November (JASON) in the North Atlantic (NAT) and the western North Pacific
5 (WNP). Extreme rain events are defined in terms of percentile rainrate, and TC-rain by
6 rainfall associated with a named TC. Results show that climatologically, 8% of rain
7 events and 17% of the total rain amount in NAT are accounted by TCs, compared to 9%
8 of rain events and 21% of rain amount in WNP. The fractional contribution of
9 accumulated TC-rain to total rain, Ω , increases nearly linearly as a function of rainrate.

10 Extending the analyses using GPCP pentad data for 1979–2005, and for the post-
11 SSM/I period (1988–2005), we find that while there is no significant trend in the total
12 JASON rainfall over NAT or WNP, there is a positive significant trend in heavy rain over
13 both basins for the 1979–2005 period, but not for the post-SSM/I period. Trend analyses
14 of Ω for both periods indicate that TCs have been feeding increasingly more to rainfall
15 extremes in NAT, where the expansion of the warm pool area can explain slight more
16 than 50% of the change in observed trend in total TC rainfall. In WNP, trend signals for
17 Ω are mixed, and the long-term relationship between TC rain and warm pool areas are
18 strongly influenced by interannual and interdecadal variability.

19

1 **Introduction**

2 Recent studies have indicated that a warming trend in sea surface temperature
3 (SST) may be responsible for increasing hurricane intensity in recent decades [Emanuel
4 2005; Webster *et al.* 2005]. Climate models have predicted increases in both storm
5 intensity and near-storm precipitation rates in a warming environment induced by
6 increasing greenhouse gases [Knutson and Tuleya 2004]. However, it is well known that
7 hurricane activity is influenced by a multitude of environmental factors including not
8 only SST [Shapiro 1982; Shapiro and Goldenberg 1998; Saunders and Harris 1997] but
9 also sea-level pressure [Landsea *et al.* 1998; Gray 1984; Knaff 1997], troposphere
10 moisture [Landsea *et al.* 1998], vertical wind shear, and stratospheric quasi-biennial
11 oscillation [Gray, 1968, 1984; Goldenberg and Shapiro 1996; Shapiro 1989; Shapiro and
12 Goldenberg 1998; Landsea *et al.* 1998]. These factors may be further influenced by
13 dominant weather and climate variabilities such as El Nino, multi-decadal oscillation,
14 African easterly wave, and West African Sahel rainfall [Gray 1990; Goldenberg et al.
15 1996, 2001; Landsea and Gray 1992; Landsea 1993; Landsea *et al.* 1994] .

16 Similarly, interannual variability of typhoon activity over the western North Pacific
17 is strongly regulated by the El Nino-Southern Oscillation through its influence on the
18 monsoon trough, low-level relative vorticity, vertical wind shear and moist static energy
19 [Chan and Liu 2004; Wang and Chan 2002]. Because of the large interannual and
20 interdecadal variabilities of factors that influence hurricane/typhoon activity, and inherent
21 uncertainties in long-term hurricane records, identifying a linkage between
22 hurricane/typhoon (hereafter collectively referred to as tropical cyclone, TC) and global

1 warming is a very challenging task [Henderson-Sellers et al. 1998; Trenberth 2005;
2 Pielke et al. 2005; Shepherd and Knutson 2006].

3 On the other hand, studies have shown that precipitation characteristics are more
4 likely subject to climate change than total precipitation amount [Trenberth 2003]. Lau
5 and Wu [2007] analyzed 25 years of satellite rainfall data and found a significant shift in
6 the rainfall distribution that indicates positive trends in extreme heavy and light rains,
7 and a negative trend in moderate rain in the tropics. Studies also show that precipitation
8 mostly in the upper percentile of the distribution over the United State has increased in
9 recent decades and that the portion of total precipitation derived from extreme and heavy
10 events increased significantly [Karl and Knight 1998; Groisman et al. 2004]. Extreme
11 rain events can arise from a variety of severe weather systems such as squall lines, meso-
12 scale convective complexes, tropical supercloud clusters, TCs and others. Given the
13 increasing evidence on the connection between extreme weather events and climate
14 change [IPCC 2007], it may be instructive to understand the linkage between TC activity
15 and climate change through the perspective of extreme rain events. Recent studies have
16 shown that TCs may have contributed to increase in extreme heavy rainfall in many
17 different regions of the world, in particular along the coastal regions of South China and
18 southeastern United States [Wu et al. 2007; Shepherd et al, 2007]. The questions we
19 address in this paper are: What are the relationships between extreme rain events and TC
20 activity? Can we detect long-term trends in current multi-decadal satellite rainfall data?
21 If so, would it be possible to infer a linkage between TC activity and SST through
22 statistics of rainfall extremes? Past studies of trends of intense TCs may have suffered
23 from uncertainties stemming from changes in the definition of TC intensity by different

1 operational centers, based on sustained maximum wind or subjective satellite imagery
2 interpretation [Velden *et al.* 2006; Landsea *et al.* 2006]. Up to now, there have been very
3 few observational studies linking possible trends in TC to tropical rainfall [Groisman et
4 al. 2004]. In this paper, we use percentile ranked rain rate from satellite rainfall data, to
5 examine possible trends in TC contribution to extreme rainfall statistics.

6

7 **2. Data and Methodology**

8 Data used in this study include the pentad rainfall from the Global Precipitation
9 Climatology Project (GPCP) for 1979–2005 [Xie et al. 2003], the 3-hourly Tropical
10 Rainfall Measurement Mission (TRMM) Multi-satellite Precipitation Analysis (TMPA)
11 data for 1998–2005 [Huffman et al., 2007], the 6-hourly best storm track data for North
12 Atlantic (NAT) [Jarvinen et al. 1984] and western North Pacific (WNP) [Chu et al.,
13 2000] for 1979–2005 from the National Hurricane Center and Joint Typhoon Warning
14 Center, respectively, with a correction of wind speed [Emanuel 2005]. The Hadley Center
15 monthly data (1979–2005) is used for the SST analysis [Rayner et al. 2003]. The 3-hourly
16 TMPA data is used to generate daily gridded precipitation data. The spatial resolution is
17 2.5° latitude x 2.5° longitude for GPCP, 0.25° x 0.25° for TRMM, and 1° x 1° for SST.
18 The analyses in this study are based on a large oceanic domain (20°W – 90°W , 10°N –
19 40°N) over NAT, and a domain with comparable size (120°E – 180°E , 10°N – 40°N) over
20 WNP during the major TC season, July through November (JASON). Following the
21 approach described in Lau and Wu [2007], we construct the probability distribution
22 function (PDF) and cumulative PDF (CPDF) of rain amount and rain frequency, with the
23 data binned at the interval of 1 mm/day. Rainfall extremes will be defined with respect to

1 ranked rain rates, as top 20% (T20), top 10% (T10), and top 5% (T5) extreme rain, from
2 the CPDFs of rain amount in each ocean domain. The results to be shown are
3 independent of the exact percentile ranks, which are only chosen as representative
4 markers to quantify the extreme rain events. Using this notation, the total rain can be
5 labeled as T100.

6 In order to examine the TC contributions to the total rain and to each rainfall
7 category, we calculate the TC-related rainfall using the 6-hourly storm track data for both
8 NAT and WNP. Following Larson *et al.* [2005] and Rodgers *et al.* [2000, 2001], we
9 define TC-rain as rain that falls within an area of 500 km radius, from the center of the
10 TC, *i.e.*, assuming that rainfall occurs within the 500 km of storm center is all associated
11 with the TC during the same day the TC occurs. This procedure is applied to the TRMM
12 daily data. Because of GPCP's coarse spatial and temporal resolutions, we define the
13 pentad rain as TC-rain if a TC passes through during anytime of the pentad within the
14 500 km of the grid box. If the pentad rain meets the criteria of extreme rain, it is further
15 defined as TC-related extreme rainfall. The GPCP TC-rain defined in this way is only a
16 crude approximation to actual TC-rain, because it may over-estimate the direct TC
17 contribution, since other forms of rain may have contributed to the total rainfall in the
18 pentad. On the other hand, it may under-estimate TC-rain contribution in extreme rain
19 categories, because some heavy TC-rain may not be counted in the extreme rainfall if the
20 corresponding GPCP pentad is not qualified as an extreme event due to GPCP's coarse
21 space-time resolution. The consistency between the TRMM-defined and GPCP-defined
22 rainfall extremes and TC-rain statistics are examined in Section 3a.

1 The GPCP pentad data used in the study is a merged product that combines
2 available surface rain gauge and operational satellite rainfall estimates to provide a state-
3 of-the-art, multi-decadal global dataset for climate studies [Adler et al., 2003; Xie et al.,
4 2003]. In view of the possible data inhomogeneity by changes in satellite rainfall
5 algorithms, especially the shift from mainly infrared-based before 1988, to addition of
6 microwave-based, Special Sensor Microwave/Imager (SSM/I) algorithms after 1988,
7 GPCP has been designed to preserve temporal homogeneity maximally. For example, it
8 did not incorporate the more recent high resolution TRMM instrument. For consistency,
9 only one SSM/I instrument is selected at a time, from satellites with early equatorial
10 crossing time (F8, F11, F13) (Ferraro, personal communication). The monthly GPCP
11 has been cross-calibrated before 1988 (pre-SSM/I) with later period (post-SSM/I) based
12 on an overlapping period to minimize the systematic bias [Adler et al., 2003]. The pentad
13 GPCP is matched to the monthly GPCP in that the pentad approximately sums to the
14 monthly estimate. However, this calibration is not likely to eliminate all the biases with
15 respect to the inhomogeneity due to the inclusion of SSM/I since 1988. Hence results
16 incorporating GPCP data for both the pre- and post-SSM/I period should be treated with
17 extreme caution. This study should be considered as a “best-effort” attempt at exploring
18 extreme rainfall trend signals, and their possible relationship with SST, using the only
19 available multi-decadal satellite rainfall data. In the following analyses, we will discuss
20 the trends derived from the entire 27-year period (1979–2005) and compare with those
21 derived from the 18-year post-SSM/I period (1988–2005) only, in order to get a better
22 assessment of the real climate trend, as well as possible data limitation.
23

1 3. Results

2

3 a) Extreme rain and TC-rain climatology

4 In this section, we discuss the basic statistics of extreme rainfall and TC-related
5 rainfall (TC-rain) based on the daily TRMM data, for NAT and WNP respectively, to
6 provide background for understanding the main results shown in Sections 3b and 3c. We
7 also examine the consistency of TRMM-derived and the GPCP-derived rain statistics for
8 the overlapping periods (1998–2005) to ensure that GPCP pentad data are good for trend
9 analysis for the extended period (1979–2005). To facilitate the analysis, we define the
10 following relationships:

$$\begin{aligned} \mathbf{AR}_{\text{TC}}(r) &= \mathbf{\Omega}(r) \mathbf{AR}(r), \\ \mathbf{AR}_{\text{TC}}(r) &\equiv \int_r^{\infty} \mathbf{R}_{\text{TC}}(r) dr, \text{ and } \mathbf{AR}(r) \equiv \int_r^{\infty} \mathbf{R}(r) dr, \end{aligned} \quad (1)$$

12 where $\mathbf{R}_{\text{TC}}(\mathbf{r})$ is the TC-rain amount, and $\mathbf{R}(\mathbf{r})$, the total rain amount for a given rainrate,
13 \mathbf{r} ; $\mathbf{AR}_{\text{TC}}(\mathbf{r})$ and $\mathbf{AR}(\mathbf{r})$, the accumulated TC-rain and accumulated total rain with
14 rainrate greater than \mathbf{r} ; $\mathbf{\Omega}(\mathbf{r})$ is a scaling factor representing the fractional contribution of
15 accumulated TC-rain to total rain. Note that from (1), the accumulated total rain, and
16 total TC-rain is denoted by $\mathbf{AR}(0)$ and $\mathbf{AR}_{\text{TC}}(0)$ respectively.

17 Figure 1a shows the CPDFs associated with total rain ($1-\mathbf{AR}(\mathbf{r})/\mathbf{AR}(0)$), TC rain ($1 -$
18 $\mathbf{AR}_{\text{TC}}(\mathbf{r})/\mathbf{AR}_{\text{TC}}(0)$), and the ratio $\mathbf{\Omega}(\mathbf{r})$ in NAT. Similar CPDFs for the rain event have
19 been constructed (Fig. 1b), with the rainfall amount replaced by the frequency of
20 occurrence (FOC) of rain events. For low rain rates, the CPDF of total rain increases
21 more rapidly than that of TC rain. For high rain rates, the reverse holds. These indicate
22 that TC contributes more to heavy rain events than to light rain events. Interestingly, the
23 percentage contribution of \mathbf{AR}_{TC} to \mathbf{AR} , as represented by the scaling factor $\mathbf{\Omega}$, increases

1 approximately linearly as a function of rain rate. As shown by the intercepts of Ω at the
2 ordinate, i.e., $\Omega(0)$ in Fig. 1a, and also in Table 1, the total TC-rain accounts for a
3 significant portion (17.3%) of the total rain amount, but occurs rather infrequently,
4 accounting for only 7.9% of the FOC (as shown by Fig. 1b). For extreme rain, for
5 example T10, 49% of rain events, and 53% of rain amount are accounted for by TC-rain
6 for NAT. These results are consistent with Shepherd et al. [2007] who found that TCs,
7 particularly stronger storms ($> \text{Cat. 3}$), contributed most to extreme rainfall (e.g. defined as Wet
8 Millimeter Days in their study) in Gulf of Mexico and East U.S. coastal areas. The percentage of
9 TC contribution to total rain is slightly higher in this study as compared to Shepherd et al. [2007]
10 and Rodgers et al. [2001], possibly due to differences in domain sizes, and study periods. For
11 WNP, the CPDFs (not shown) are similar, including the nearly linear increase in Ω with
12 rainrate. Our estimates of WNP TC-rainfall are also comparable to those of Wu et al. [2007] and
13 Rodgers et al. [2000]. The key CPDF statistics for NAT and WNP are shown in Table 1.
14 Comparing the Ω factors in the two domains, the TCs in WNP appear to produce more
15 intense rain than in NAT, accounting for 9.0% of rain occurrence, but 20.6% of the total
16 rain amount. The higher rainfall intensity for WNP TCs is also reflected in the higher
17 rainfall thresholds in all three extreme rain categories (T5, T10 and T20). At T10 for
18 WNP, TC-rain accounts for 53% rain events and 57% rain amount. At T5, the
19 corresponding ratios are 62% and 64%. The Ω factors appear to approach a common
20 value ($\sim 65\%$ for T5 rain amount) for highly extreme events for both domains. This
21 means that even at such highly extreme rain events, non-TC-rain can still contribute no
22 less than 30% of the rain amount.

23 Similar CPDFs are constructed from GPCP data for the overlapping period of the
24 two datasets (1998–2005). For comparison, the statistics for GPCP-defined extreme

1 events are shown in Tables 2a and 2b for NAT, and WNP respectively. Since the GPCP
2 pentad rainfall has lower spatial and temporal resolutions compared to TRMM, TC-rain
3 can only be defined for the entire pentad, i.e., counting all rainfall within a pentad, if a
4 TC passes over a given location during anytime of the pentad. Comparing Table 2 to
5 Table 1, it is clear that the even though the thresholds for the GPCP extreme events are
6 considerably lower relative to those for the daily TRMM data, the Ω factors are
7 reasonably scale-invariant with respect to the extreme categories, with increasing TC
8 contributions for heavier rains.

9 The spatial distributions of TC-rain (Fig. 2) for a 5-day period during Hurricane
10 Katrina (Aug 24–28, 2005) and during Typhoons Talim and Nabi (Aug 29 – Sep 2, 2005)
11 show good match in patterns and relative magnitudes between the GPCP-pentad rain and
12 the 5-day rain constructed from the TRMM 3-hourly data, indicating that both datasets
13 captured essentially the same TC-related rain systems. The distributions shown are
14 typical of many other TC events we have examined. The above results provide some
15 reassurance that the GPCP data can be used to study the relationship between extreme
16 rain and TC-rain, for the extended period of the GPCP.

17 *b) Trends in rainfall characteristics*

18 As demonstrated by previous studies, trends in rainfall characteristics may be
19 manifested as shifts in the rainfall PDF. For the JASON season, a shift in the rainfall
20 PDF from the first half (1979–1991) of the data record to the second half (1993–2005) is
21 apparent for both domains (Figs. 3a and c). The latter period shows increasing heavy
22 rains, and decreasing moderate rains compared to the earlier. The strong signal in the
23 extreme rain can be seen more clearly in the normalized deviation (difference between

1 second and first periods divided by the mean of the two periods) for each rain bin (Figs.
2 3b and d), which show clearly positive increments for heavy rain events with some very
3 large ($> 50\%$) deviations for very extreme events (T5 or above). The relative changes
4 appear to be more pronounced in NAT compared to WNP. For NAT, positive trends are
5 found for all heavy rain with rainrate greater than ~ 14 mm/day. For WNP, the
6 corresponding rain-rate is ~ 20 mm/day. These values correspond to the rain-rate
7 thresholds for T20 rain category in the two ocean domains, respectively (see Table 2). A
8 compensating negative trend in moderate-to-light rains ($2\text{--}15$ mm day $^{-1}$) is obvious in
9 both domains.

10 To examine the long-term variations of total rain, extreme rain, and associated TC
11 contributions, we have constructed the time series of the seasonal (JASON) $\mathbf{AR}(\mathbf{r})$, and
12 $\mathbf{AR}_{TC}(\mathbf{r})$ for the entire data period (1979–2005) for different threshold values of \mathbf{r} , that
13 correspond to total rain ($\mathbf{r}=0$), and to rainrate threshold (see Table 2) for extreme rain
14 categories, T20, T10 and T5 respectively. Similarly, the accumulated FOC for the same
15 rain categories have been computed. To suppress effects of El Nino Southern Oscillation
16 (ENSO), and to highlight the long-term behavior, a 5-year running mean has been applied
17 and the resulting time series are shown as thick solid or dashed lines in Figs. 4 and 5. A
18 vertical dash line is also drawn in each figure to mark the boundary between the pre-
19 SSM/I and post-SSM/I periods. In the following, a time series is considered to possess a
20 trend when its linear regression exceeds the 95% confidence level (c.l.), computed based
21 on the R^2 statistical test [Wilks 1995]. As shown in Fig. 4a, in NAT, while the domain-
22 average total GPCP rainfall, $\mathbf{AR}(0)$ (labeled as all-event in Fig. 4a), possesses no
23 discernible trend, a trend exists in total TC-rain $\mathbf{AR}_{TC}(0)$, especially for the post-SSM/I

1 period. Fig. 4b shows that the TC-rain possesses a significant trend in FOC, with strong
2 signals coming from the post-SSM/I period. The accumulated TC rain intensity, **ARI**,
3 defined as the \mathbf{AR}_{TC} divided by FOC, shows a positive trend for the entire period, but
4 only a weak indication of a trend for the post-SSM/I period. In contrast, in WNP, both
5 the total rain, $\mathbf{AR}(0)$, and total TC-rain amount, $\mathbf{AR}_{TC}(0)$, show large decadal scale
6 swings, and exhibit no obvious trends (Fig. 4c). Notice also that $\mathbf{AR}(0)$ and $\mathbf{AR}_{TC}(0)$ in
7 WNP are much higher than in NAT, with the TCs in the WNP producing more than
8 double the rain amount in NAT. For WNP, TC-rain does not, shown a significant trend
9 in FOC for the whole period. However, the **ARI** shows a slight positive trend (Fig. 4d)
10 for the whole period, indicating a possible increase in rainfall intensity associated with
11 TCs. As we will show later, the FOC seems to dominate the variation of TC contribution
12 to extreme rain events. The results for trend analysis for extreme events are presented
13 next.

14 Since all three extreme rain categories have similar variability, only those for T10
15 are shown (Fig. 5). For NAT, the T10 **AR** and \mathbf{AR}_{TC} show large interannual and decadal
16 variations with peaks in the late 1980s and mid-1990s and lows in the early 1980s (Fig.
17 5a). Significant upward trends ($> 99\%$ c.l.) are observed for both **AR** and \mathbf{AR}_{TC} for the
18 whole period. However, the trends are weaker in the post-SSM/I period (see also the
19 discussion for Table 3). The residual (figure omitted) computed as the difference
20 between the two time series shows no clear long-term signal. Hence, it can be inferred
21 that the TCs are feeding dominantly to the variability and trend of **AR** for T10. Fig. 5b
22 shows that for T10, FOC also has a clear trend ($>99\%$ c.l.), similar to **AR** and \mathbf{AR}_{TC} .
23 There is a less pronounced trend in **ARI** for TC in this rain category (dotted line in Fig.

1 5b). Both trends may have been contributed by suppressed activities during the pre-
2 SSM/I period. For the post-SSM/I period, positive trends are still discernible, but much
3 weaker. Regardless of the time period, the stronger trend in TC FOC, and its similarity in
4 variations to **AR** imply that the observed trend in extreme rain amount (Fig. 5a) is likely
5 to be derived primarily from more TC events (either more TCs or TCs with longer
6 duration), and to a less degree from an increase in TC intensity.

7 For WNP, large interannual and decadal variations dominate both **AR** and **AR_{TC}**
8 for T10 (Fig. 5c). The **AR** rises relatively steeply from 1984 to 1989, and stays nearly
9 constant with a slight decline from 1995–2005. The **AR_{TC}** shows a similar rapid rise
10 from the mid-1980s to the mid-1990s, followed by a more pronounced decline after 1995.
11 The increasing number of WNP TCs from 1980 and the steep rise in mid-1980s to mid-
12 1990s are reported in [Chan and Shi, 1996] and [Chan and Liu 2004], respectively. As a
13 result, although both **AR** and **AR_{TC}** show significant linear trends for the entire period,
14 much of the signal may be attributed to the pre-SSM/I period, possibly as part of a
15 decadal-scale variation, and/or due to inhomogeneity between the pre- and post-SSM/I
16 data (see further discussion for Table 3). The closeness of the two time series suggests
17 that TCs contribute strongly to the variability and trend of the extreme rain event in
18 WPN. The FOC time series for T10_**TC** events (Fig. 5d) shows long-term variations
19 similar to the T10 rain amount (solid curve in Fig. 5c), suggesting that variations in
20 extreme rain may be due to TC events. The TC **ARI** for T10 in WNP also shows an
21 apparent positive trend, but with much of the signal coming from the pre-SSM/I period.
22 *c) Relationships with SST*

1 Previous studies have noted that NAT and WNP have been warming at a
2 moderate rate of approximately 0.5°C or less from 1980 through 2005 [e.g., Webster et
3 al. 2005]. Because of the strong control by surface evaporation on TC intensity [Emanuel
4 1987], and that TCs are seldom formed when SST is below 26°C , it has been suggested
5 that TC activity may be sensitive to the area of the warm pool [Wang et al. 2006]. This
6 suggestion has yet to be confirmed by climate models because of the complex factors
7 affecting tropical cyclogenesis. For example, the NCAR CSM1 predicts that the
8 threshold SST for tropical deep convection in a warmer climate may also increase, hence
9 expanding the 26°C isotherm is likely to have little effect on areal extent of cyclogenesis
10 [Dutton et al., 2000], while others [Wang et al., 2008] found reduced tropospheric
11 vertical wind shear in the main hurricane development region, and increased moist static
12 instability of troposphere in the presence of a larger north Atlantic warm pool, both of
13 which favor the intensification of tropical storms into major hurricanes. Here we will
14 examine the relation of SST warm pool area with TC related rainfall and extreme rain.
15 The warming signals in NAT and WNP are most pronounced at the higher SSTs as
16 evidenced in the PDF of SST constructed using a 0.5°C bin for two ocean basins in
17 JASON for the first (pre-1992) and the second half (post-1992) periods (Fig.6). In
18 NAT (Figs. 6a and b) there is a clear signal of increase in FOC of SST $>28\text{--}29^{\circ}\text{C}$, and
19 decreased occurrence of cooler SST ($<28^{\circ}\text{C}$). Similar shifts in the SST PDF can be
20 found in WNP (Figs. 6c and d). If we define the size of the warm pool as areas with SST
21 $> 28^{\circ}\text{C}$, the PDF shift translates into an increase in total warm pool area of approximately
22 14% per-decade in NAT, and only 6% per-decade in WNP respectively for the entire
23 period (Table 3).

1 Fig. 7 shows the relationship between the warm pool area and the fractional
2 contribution of TC-rain to total rain, i.e., the Ω factor in Eq. 1 for T10. In NAT (Fig.
3 7a), Ω for T10 shows a pronounced upward trend for the entire period, indicating an
4 increasing TC contribution to extreme rain amount. The long-term variation of Ω tracks
5 well the percentage change in the area of the warm pool, suggesting a possible
6 relationship between TC-rain contribution to extreme rain events and the relative size of
7 the warm pool. The positive trends appear to begin in 1984-85, indicating increasing TC
8 contribution to extreme rainfall associated with a substantially expanded warm pool in
9 NAT in the last two decades. By comparison, Ω in WNP (Fig. 7b) increases only
10 modestly with large decadal-scale variation. This modest overall increase in TC-rain
11 contribution is consistent with the smaller percentage increase in warm pool size in WNP
12 compared to NAT, during the same periods.

13 In the following, we provide a summary of the main results and a discussion of
14 possible influences due to inclusion of the pre-SSM/I period. From Table 3, for NAT,
15 there are positive trends for total TC-rain (24.9 mm/decade). This is a substantial rate
16 approximately equal to 41% per-decade change in the mean. Here, all extreme rain
17 categories (T20, through T5) show significant increase ranging from 14.8 to 7.4
18 mm/decade, or approximately 57-75% per-decade change in the mean. These trends are
19 highly significant (>99% c.l.) for the entire data period. When the pre-SSM/I periods are
20 excluded, only the total TC-rain remains significant (>95% c.l.). Here, the trends for TC
21 related T20, T10 and T5 extreme rains remain positive in the 11.3 to 4.8 mm /decade
22 range, which corresponds approximately to 32-34% per-decade change in the mean. The
23 drop in signal using post-SSM/I data may be due to sampling errors from the shorter

1 record, and/or due to possible influence of data inhomogeneity between the pre- and post-
2 SSM/I periods. Notably, the fractional contribution of TC in extreme rain, Ω , indicates a
3 positive trend in the range of 12-18% per-decade for all extreme rainfall categories, when
4 computed using data for the entire period. Using post-SSM/I data only, the magnitudes
5 of the Ω trends are comparable at a range of 11-15% per-decade. These trends are only
6 marginally significant ($> 90\%$ c.l.), possibly due to reduced degree of freedom in the
7 shorter data record. The consistent increase of Ω for increasing extreme rain categories
8 for both data periods suggest a minimal impact of data inhomogeneity, because the ratio
9 of extreme rain to total rain may be less sensitive to the different rainfall algorithms used
10 in the GPCP data. With respect to SST, separate computation shows a significant
11 correlation (0.53 for T10) with the size of warm pool which is expanding at 14% per-
12 decade over the entire period. This correlation increases slightly to 0.55 for the post-
13 SSM/I period, when the NAT warm pool is expanding at 22%. Detrending both time
14 series, the correlations are reduced to 0.26 for the entire period, and to 0.41 for the post-
15 SSM/I period, indicating that a significant portion of the correlation between Ω and the
16 warm pool area is contributed by the linear trend.

17 In WNP, large interannual and decadal oscillation dominate the TC activity with
18 peaks in the mid-1990's which coincide with the first half of the post-SSM/I era (see also
19 Fig. 4d). Trend signals computed in WNP are masked by the dominant decadal variation.
20 For example, the positive trends in extreme rain categories computed from the whole data
21 period that range from 26.0 to 15.1 mm/decade for T20 through T5 (Table 3), are likely
22 due to the steep rise in TC activities from the mid-1980s to mid-1990s noted in previous
23 discussions (see Fig. 5d). The corresponding change in Ω is approximately constant at 3-

1 4% for all extreme rain categories. For the post-SSM/I period only, the negative and
2 small trend signals for all extreme rain statistics are again most likely related to the
3 negative swing of the decadal variation in TC activities in the WNP since 1995.
4 Notwithstanding the decline in total TC rain and T20_TC rain, Ω for T10 and T5 still
5 increases at 3% per-decade in the post-SSM/I period. These trends are, however, not
6 significant (<95% c.l.), being masked by large interannual and interdecadal variability.
7 Also worth noting is the smaller change of warm pool area in WNP (6% per-decade for
8 the entire period and 9% for the post-SSM/I period), compared to NAT. There are weak
9 negative correlations (-0.22) between Ω_{T10} and the warm pool area for the entire
10 period, and (- 0.28) during the post-SSM/I period, both are insignificant at the 95% c.l.
11 level. Detrending the time series increases the negative correlation to -0.58 (>95% c.l.)
12 for the entire period, and -0.59 (>95% c.l.) for the post-SSM/I period. The higher
13 correlations after detrending are most likely indicative of the strong control of ENSO and
14 related coupled ocean-atmosphere interactions in WNP. In both ocean basins, clearly the
15 linear trend is affected by interannual/interdecadal variability of the warm pool area,
16 especially for WNP, where such variability may have masked any trend signals in the
17 extreme rainfall statistics.

18 *d) Comparison with previous work*

19 Recently, Emanuel [2005] and Webster et al. [2005] found nearly doubling of the
20 number of intense TCs (Categories 4 and 5 based on the Saffir-Simpson scale) in both
21 NAT and WNP. However, Klotzbach [2006] found a much smaller trend of about 10%
22 globally in Categories 4 and 5, and a large increase in Categories 4 and 5 in NAT, but not
23 in WNP. Kossin et al. [2007] reported that there are no robust trends in intense TCs in all

1 ocean basins, except for the North Atlantic since 1983. Our results are consistent with
2 these authors in that for most TC rainfall statistics, significant trends are found in NAT,
3 but only mixed signals are found in WNP. The difference in trend signals between the
4 two oceans may be related to the differences in the rate of expansion of the warm pools
5 (SST >28°C), and in the underlying relationship with the atmosphere and warm pool
6 SST. Based on the regression of total TC rain and warm pool area, we found that an
7 increase of approximately 13 mm per decade of total TC rain can be expected from the
8 observed expansion rate (14% per decade) of the warm pool in NAT. This means that
9 slightly more than 50% of the observed increased in TC rain (24.9 mm, as shown in
10 Table 3) can be explained by increase in warm pool area in NAT. For the WNP, the
11 relationship between the warm pool area and total TC rain is dominated by the decadal
12 and ENSO variability, and no significant signals in TC total rain can be attributed to SST
13 trends. While we have found increased rainfall contribution by active TC activity
14 associated with the expansion of warm pool in NAT using GPCP data, we cannot address
15 or extrapolate our results for the pre-satellite period, e.g., active TC activity in NAT
16 during late 1920s and late 1960s [Goldenberg et al. 2001]. For WNP, the GPCP record
17 length may still be too short to extract significant trend signals.

18 Our approach differs from previous studies in that we focus on detecting TC
19 extreme rainfall trend signals over the tropical oceans using multi-decadal satellite
20 rainfall data from GPCP. We used a unified classification of rain extremes and TC-rain
21 in both oceans. Hence, our definition of TC-rain is not subject to the uncertainties due to
22 secular changes in the definition of TC intensity used by different operational centers. By
23 definition, the contribution of TC-rain to accumulated extreme rain, Ω , is an integral

1 property and a ratio that is a more stable quantity compared to TC intensity defined for
2 individual storms, and is therefore less sensitive to inhomogeneity in GPCP data due to
3 different instruments mix between the pre-SSM/I and post-SSM/I periods. Our results are
4 consistent with recent high-resolution global modeling experiments indicating increase in
5 number of simulated high-intensity TCs under warmer SST and higher specific humidity
6 conditions [Bengtsson et al., 2007]. The increasing hurricane rainfall and rainfall
7 intensity in NAT is also consistent with the modeling study of Knutson and Tuleya
8 [2004], and observational study of Lonfat et al. [2004] where they showed increasing rain
9 rates with increasing tropical cyclone intensity.

10 **4. Conclusions**

11 Using TRMM and GPCP data, we have documented the mean and long-term
12 changes in the contribution of TCs to rainfall as a function of rain rates in NAT, and
13 WNP. We find that during the TC season, July–November, TC accounts for
14 approximately 8% of the total rain events, but about 17% of the rainfall amount in NAT,
15 as compared to 9% of rain events and 21% of rainfall amount in WNP based on TRMM
16 data from 1998 to 2005. Overall, TCs in WNP appear to be more energetic than NAT in
17 terms of having higher average rainfall intensity, and higher rainfall thresholds for given
18 percentile extreme rain rates. Using the full record (1979-2005) GPCP data, we find a
19 substantial shift in the rainfall PDF during the TC season, manifested as an increase in
20 extreme rain amount and events in both oceans. However, with regard to the
21 relationships between TCs and extreme rain, substantial differences are found between
22 the two ocean domains, especially when the pre-SSM/I data are excluded. In NAT, the
23 contributions of TC to the top extreme rainfall are increasing at 12–18% per-decade, and

1 at a comparable rate of 11–15% per-decade for post-SSM/I period. In contrast, WNP
2 TCs only contribute to a modest increase of about 3–4% per-decade in extreme rain. Our
3 results suggest that TCs are contributing increasingly more in rainfall extreme events in
4 the past two decades in NAT. However, in WNP, the trend signals are mixed because of
5 the larger influences of interannual and decadal variations and possibly inhomogeneity in
6 the GPCP data. We speculate that the different rate of increase may be related to the
7 larger percentage increase in the size of the warm pool in NAT compared to WNP, as
8 well as to the large-scale circulation and moisture conditions pertaining to each ocean
9 basin. This is consistent with a recent study [Vecchi and Soden 2007] which suggests
10 that tropical cyclone potential intensity is more sensitive to localized SST changes
11 stemming from coupled ocean-atmosphere dynamical feedback, than to the uniform SST
12 pattern associated with greenhouse-gas-induced warming.

13 Obviously, the results in this work are subject to uncertainties in the satellite
14 rainfall data. We have shown that the temporal inhomogeneity in GPCP data from the
15 pre-SSM/I and post-SSM/I period may affect some of the derived trends. Our study
16 suggests that useful climate signals could be detected for extreme rainfall statistics from
17 the GPCP data. It also demonstrates the need for realistic error estimates with respect to
18 data inhomogeneity in multi-decadal global satellite data, and cross-validation with
19 model results. Finally, our results are consistent with the notion that regional climate
20 change signals tend to manifest themselves in statistics of extreme events, rather than in
21 changes in the mean. Efforts are now underway to extend this study to other ocean
22 basins and to examine different parts of the spectrum and their relationship to rainfall
23 characteristics and associated weather phenomena and climate processes. These efforts

1 underscore the need for extending and improving long-term rainfall datasets to obtain
2 reliable estimates of rainfall PDFs, such as those anticipated by the Global Precipitation
3 Measurement (GPM) program [Smith et al., 2007]. The continuation of TRMM data into
4 the GPM era, and the continuously reprocessing of satellite data are critical for
5 quantitative assessment of the role of rainfall on the atmospheric water cycle associated
6 with climate change.

7
8 **Acknowledgement.** This work is supported by the Precipitation Measuring Mission
9 (Headquarter Manager: Dr. R. Kakar), NASA Earth Science Division. We thank **Dr.**
10 **Chris Landsea** and two anonymous reviewers for constructive comments that have
11 improved the manuscript.

1

2 **References:**

3 Adler, R. F. and Coauthors (2003), The version-2 Global Precipitation Climatology
4 Project (GPCP) monthly precipitation analysis (1979–present), *J. Hydrometeor.*, 4,
5 1147–1167.

6 Bengtsson, L. K. I. Hodges, M. Esch, N. Keenlyside, L. Kornblueh, J. J. Luo, and T.
7 Yamagata (2007), How may tropical cyclone change in a warmer climate? Submitted
8 to *Tellus*.

9 Chan, J. C. L. and K. S. Liu (2004), Global warming and western North Pacific typhoon
10 activity from an observational perspective. *J. Clim.*, 17, 4590–4602.

11 Chu, J.-H., C. R. Sampson, A. S. Levine, E. Fukada (2002), The Joint Typhoon Warning
12 Center Tropical Cyclone Best-Tracks, 1945-2000. NRL Reference Number: NRL
13 /MR/7540-02-16. http://metocph.nmci.navy.mil/jtwc/best_tracks/TC_bt_report.html

14 Dutton, J. F., C. J. Poulsen, and J. L. Evans (2000), The effect of global climate change
15 on the regions of tropical convection in CSM1. *Geophys. Res. Letters*, 27, 3049.

16 Emanuel, K.A. (1987), The dependence of hurricane intensity on climate. *Nature*, 326,
17 483–485.

18 Emanuel, K. (2005), Increasing destructiveness of tropical cyclones over the past 30
19 years, *Nature*, 436, 686–688.

20 Goldenberg S. B., and L. J. Shapiro (1996), Physical mechanisms for the association of
21 El Niño and West African rainfall with Atlantic major hurricane activity. *J. Climate*,
22 9, 1169–1187.

23 Goldenberg, S. B., C. Landsea, A. M. Mestas-Nuñez, and W. M. Gray (2001), The recent
24 increase in Atlantic hurricane activity. *Science*, 293, 474–479.

1 Gray W. M. (1968), Global view of the origin of tropical disturbances and storms. *Mon.*
2 *Wea. Rev.*, 96, 669–700.

3 Gray W. M. (1984), Atlantic seasonal hurricane frequency. Part I: El Niño and 30 mb
4 quasi-biennial oscillation influences. *Mon. Wea. Rev.*, 112, 1649–1668.

5 Gray W. M. (1990), Strong association between West African rainfall and U.S. landfall
6 of intense hurricanes. *Science*, 249, 1251–1256.

7 Groisman, P. Y, et al., 2004: Contemporary changes of the hydrological cycle over the
8 contiguous United States: trends derived from in situ observations. *J.*
9 *Hydrometeorology*, 5, 64-85.

10 Henderson-Sellers, A., H. Zhang, G. Berz, K. Emanuel, W. Gray, C. Landsea, G.
11 Holland, J. Lighthill, S-L. Shieh, P. Webster, K. McGuffie (1998). Tropical cyclones
12 and global climate change: A post-IPCC assessment. *Bull. Amer. Meteor. Soc.*, 79,
13 19-38.

14 Huffman, G., R. F. Adler, D. T. Bolvin, G. Gu, E. J. Nelkin, K. P. Bowman, Y.
15 Hong, E. F. Stocker, and D. B. Wolff (2007), The TRMM multisatellite precipitation
16 analysis (TMPA): quasi-global, multiyear, combined-sensor precipitation estimates at
17 fine scales, *J. Hydrometeor.*, 8, 38–55.

18 IPCC, 2007: *Climate Change 2007: The Physical Science Basis*. Contribution of Working
19 Group I to the Fourth Assessment Report of the Intergovernmental Panel on Climate
20 Change [Solomon, S., D. Qin, M. Manning, Z. Chen, M. Marquis, K.B. Averyt, M.
21 Tignor and H.L. Miller (eds.)]. Cambridge University Press, Cambridge, United
22 Kingdom and New York, NY, USA, 996 pp.

1 Jarvinen, B. R., C. J. Neumann, and M. A. S. Davis (1984), A tropical
2 cyclone data tape for the North Atlantic Basin, 1886-1983: Contents, limitations, and
3 uses. NOAA Technical Memorandum NWS NHC 22, Coral Gables, Florida, 21 pp.
4 <http://www.nhc.noaa.gov/pdf/NWS-NHC-1988-22.pdf>

5 Karl, T. R. and R. W. Knight (1998), Secular trends of precipitation amount, frequency,
6 and intensity in the United States. *Bull. Am. Meteorol. Soc.*, 79, 231–241.

7 Klotzbach P. J. (2006), Trends in global tropical cyclone activity over the past twenty
8 years (1986–2005), *Geophys. Res. Lett.*, 33, L10805, doi:10.1029/2006GL025881.

9 Knaff J. A. (1997), Implications of summertime sea level pressure anomalies in the
10 tropical Atlantic region. *J. Clim.*, 10, 789–804.

11 Knutson, T. R., and R. E. Tuleya (2004), Impact of CO₂-induced warming on simulated
12 hurricane intensity and precipitation: Sensitivity to the choice of climate model and
13 convective parameterization. *J. Clim.*, 17, 3477–3495.

14 Kossin, J. P., K. R. Knapp, D. J. Vimont, R. J. Murnane, and B. A. Harper (2007), A
15 globally consistent reanalysis of hurricane variability and trends. *Geophys. Res. Lett.*,
16 34, L04815, doi:10.1029/2006GL028836.

17 Landsea, C. W. and W. M. Gray (1992), The strong association between Western Sahel
18 monsoon rainfall and intense Atlantic hurricanes. *J. Clim.*, 5, 435–453.

19 Landsea, C. W. (1993), A climatology of intense (or major) Atlantic hurricanes. *Mon.*
20 *Wea. Rev.*, 121, 1703–1713.

21 Landsea, C. W., W. M. Gray, P. W. Mielke, Jr., and K. J. Berry (1994), Seasonal
22 forecasting of Atlantic hurricane activity. *Weather*, 49, 273–283.

1 Landsea, C. W., G. D. Bell, W. M. Gray, S. B. Goldenberg (1998), The extremely active
2 1995 Atlantic hurricane season: environmental conditions and verification of seasonal
3 forecasts. *Mon. Wea. Rev.*, 126, 1174–1193.

4 Landsea, C. W., B. A. Harper, K. Hoarau, and J. A. Knaff (2006), Can we detect trends in
5 extreme tropical cyclones? *Science*, 313, 452–454.

6 Larson, J., Y. Zhou, and R. W. Higgins (2005), Characteristics of landfalling tropical
7 cyclones in the United States and Mexico: climatology and interannual variability. *J.*
8 *Clim.*, 18, 1247–1262.

9 Lau, K. M., and H. T. Wu (2007), Detecting trends in tropical rainfall characteristics,
10 1979-2003. *Int. J. Climatol.*, 27, 979–988.

11 Lonfat, M., F. D. Marks, Jr., and S. S. Chen (2004), Precipitation
12 distribution in tropical cyclones using the Tropical Rainfall Measuring
13 Mission (TRMM) microwave imager: A global perspective. *Mon. Wea. Rev.*,
14 132, 1645-1660.

15 Pielke, R. A., Jr., C. Landsea, M. Mayfield, J. Laver, and R. Pasch (2005), Hurricanes
16 and global warming. *Bull. Am. Meteorol. Soc.*, 86, 1571–1575.

17 Rayner, N. A., D. E. Parker, E. B. Horton, C. K. Folland, L. V. Alexander, D. P. Rowell,
18 E. C. Kent, and A. Kaplan (2003), Global analyses of SST, sea ice and night marine
19 air temperature since the late nineteenth century. *J. Geophys. Res.*, **108**, 4407,
20 doi:10.1029/2002JD002670.

21 Rodgers, E. B., R.F. Adler and H. F. Pierce (2000), Contribution of tropical cyclones to
22 the North Pacific climatological rainfall as observed from satellites. *J. Appl. Meteor.*,
23 39, 1658-1678.

1 Rodgers, E.B., R.F. Adler, and H.F. Pierce (2001), Contribution of Tropical Cyclones to
2 the North Atlantic Climatological Rainfall as Observed from Satellites. *J. Appl.*
3 *Meteor.*, **40**, 1785–1800.

4 Saunders M. A., and A. R. Harris (1997), Statistical evidence links exceptional 1995
5 Atlantic hurricane season to record sea warming. *Geophys. Res. Lett.*, **24**, 1255–1258.

6 Shapiro, L. J. (1982), Hurricane climatic fluctuations. Part II: Relation to large-scale
7 circulation. *Mon. Wea. Rev.*, **110**, 1014–1023.

8 Shapiro, L. J. (1987), Month-to-month variability of the Atlantic tropical circulation and
9 its relationship to tropical storm formation. *Mon. Wea. Rev.* **115**, 2598–2614.

10 Shapiro, L. J. (1989), The relationship of the quasi-biennial oscillation to Atlantic tropical
11 storm activity. *Mon. Wea. Rev.*, **117**, 2598–261413.

12 Shapiro, L. J. and S. B. Goldenberg (1998), Atlantic sea surface temperatures and tropical
13 cyclone formation. *J. Clim.*, **11**, 578–590.

14 Shepherd, J.M., and T. Knutson, 2006: The current debate on the linkage between global
15 warming and hurricanes, *Geography Compass*, *Geography Compass*, *Geography Compass* **1**
16 **(1)**, 1–24. doi:10.1111/j.1749-8198.2006.00002.x.

17 Shepherd, J. M., A. Grundstein, and T. L. Mote (2007), Quantifying the contribution of tropical
18 cyclones to extreme rainfall along the coastal southeastern United States, *Geophys. Res. Lett.*,
19 **34**, L23810, doi:10.1029/2007GL031694

20 Smith, E. A., and coauthors (2007), International Global Precipitation Measurement
21 (GPM) program and mission: An overview. *Measuring Precipitation from Space:*
22 *EURAINSAT and the Future*, V. Levizzani, P. Bauer, and F. J. Turk, Eds., Springer,
23 611-654.

24 Trenberth K. E., A. Dai, R. M. Rasmussen, and D. B. Parsons (2003), The changing
25 character of precipitation. *Bull. Amer. Meteor. Soc.*, **84**, 1205–1217.

- 1 Trenberth, K. (2005), Uncertainty in hurricanes and global warming, *Science*, 308, 1753–
2 1754.
- 3 Vecchi, G. A. and B. J. Soden (2007), Effect of remote sea surface temperature change
4 on tropical cyclone potential intensity. *Nature*, 450, 1066–1070.
- 5 Velden, C., et al. (2006), The Dvorak tropical cyclone intensity estimation technique: A
6 satellite-based method that has endured for over 30 years. *Bull. Am. Meteorol. Soc.*,
7 87, 1195–1210.
- 8 Wang, B., and J. C. L. Chan (2002), How strong ENSO events affect tropical storm
9 activity over the western North Pacific. *J. Clim.*, 15, 1643–1658.
- 10 Wang, C. Z., D. B. Enfield, S. K. Lee and C. W. Landsea (2006), Influences of the
11 Atlantic warm pool on western hemisphere summer rainfall and Atlantic hurricanes.
12 *J. Clim.*, 19, 3011–3028.
- 13 Wang, Chunzai, S. K. Lee and D. B. Enfield (2007), Climate response to anomalously
14 larger and small Atlantic warm pools during the summer. *J. Climat.*, 21, 2437-2450.
- 15 Webster, P. J., G. J. Holland, J. A. Curry, and H.-R. Chang (2005), Changes in tropical
16 cyclone number, duration, and intensity in a warming environment. *Science*, 309,
17 1844–1846.
- 18 Wilks, D. S. (1995), *Statistic methods in the atmospheric sciences*. Academic Press, New
19 York, 160–176.
- 20 Wu, Y. S., and P. Zhai (2007), The impact of tropical cyclones on Hainan Island’s
21 extreme and total precipitation. *Int. J. Climatol.*, 27, 1059–1064.

1 Xie P., J. E. Janowiak, P. A. Arkin, R. F. Adler, A. Gruber, R. Ferraro, G. J. Huffman,
2 and S. Curtis (2003), GPCP pentad precipitation analyses: An experimental dataset
3 based on gauge observations and satellite estimates. *J. Clim.*, 16, 2197–2214.

4

1

2 Table 1a. TC related extreme event rainfall statistics based on TRMM data for NAT
3 (90°W-20°W, 10°N-40°N) during JASON 1998-2005. Statistics are area weighted. Ω -
4 event and Ω -amount indicate the fractional contributions of cumulative TC to total rain
5 for rain event and rain amount (see text for definition), respectively,

	T5	T10	T20	TOTAL
TRMM-threshold (mm/day)	119.0	88.0	60.0	---
Ω -event (%)	61.3	49.4	36.7	7.9
Ω -amount (%)	63.9	53.2	41.6	17.3

6

7 Table 1b. Same as in Table 1a, except for WNP (120°E-180°E, 10°N-40°N).

	T5	T10	T20	Total
TRMM-threshold (mm/day)	136.0	101.0	69.0	---
Ω -events (%)	61.5	53.2	42.5	9.0
Ω -amount (%)	64.2	56.7	46.9	20.6

8

1 Table 2a. Same as in Table 1a for NAT, except for using GPCP pentad data.

	T5	T10	T20	Total
GPCP-threshold (mm/day)	23.0	18.0	13.0	---
Ω -event (%)	54.6	45.4	35.8	9.7
Ω -amount (%)	55.9	47.8	39.3	19.6

2

3 Table 2b. Same as in Table 1b for WNP, except for using GPCP pentad data.

	T5	T10	T20	Total
GPCP-threshold (mm/day)	33.0	26.0	19.0	---
Ω -events (%)	77.1	68.4	55.7	12.2
Ω -amount (%)	78.3	70.3	59.3	27.2

4

1 Table 3. Linear regression expressed as change per decade of July–November TC rain
 2 amount and its fractional contribution (Ω) in different rain categories based on the 1979–
 3 2005 and 1988–2005 data, respectively, for (a) NAT, and (b) WNP. Also shown is the
 4 change in the ratio of warm pool (SST>28° C) area to total area (second last row). Values
 5 exceeding 95% significance level are highlighted in bold. Asterisks indicate greater than
 6 99% significance. Values with marginal (~90%) significance level are underlined.
 7

a. North Atlantic	1979–2005	1988–2005
T100-TC	* 24.9 mm	29.2 mm
T20-TC	* 14.8 mm	11.3 mm
T10-TC	* 11.1 mm	7.3 mm
T5-TC	* 7.4 mm	4.8 mm
Ω -T20 (%)	* 12 %	<u>11 %</u>
Ω -T10 (%)	* 15 %	<u>13 %</u>
Ω -T5 (%)	* 18 %	<u>15 %</u>
warm pool area	* 14 %	* 22 %

8

b. North Western Pacific	1979–2005	1988–2005
T100-TC	23.6 mm	-43.2 mm
T20-TC	* 26.0 mm	-6.8 mm
T10-TC	* 23.4 mm	0.8 mm
T5-TC	* 15.1 mm	0.8 mm
Ω -T20 (%)	3 %	-1 %
Ω -T10 (%)	4 %	3 %
Ω -T5 (%)	4 %	3 %
warm pool area	* 6 %	* 9 %

9

1

2 **Figure Captions**

3 Figure 1. Cumulative PDF of daily rainfall (solid line), AR, and TC-rain (dash-dot line),
4 ARTC, from TRMM data for NAT during JASON, 1998–2005, for (a) rainfall
5 amount and (b) frequency of occurrence. The dashed line in (a) shows the
6 fractional TC-rain to total rain amount, Ω , and in (b) the fractional TC events to
7 total rain events.

8 Figure 2. TC-rain from (a) TRMM and (b) GPCP during Aug 24–28, 2005 overlay with
9 best track of Hurricane Katrina. TC-rain from (c) TRMM and (d) GPCP during Aug
10 29 – Sep 2, 2005 overlay with best tracks of Typhoons Nabi and Talim.

11 Figure 3. (a) The climatological PDF from GPCP for JASON accumulated rainfall
12 amount at each rainfall bin (with 1 mm/day interval) of the first 13 years (1979–
13 1991, outlined bar) and the latter 13 years (1993–2005, filled bar), and (b) shift in
14 PDF shown as the difference between the rainfall PDF of the latter period (1993–
15 2005) and the first period (1979–1991) normalized by the mean of these two
16 periods, for NAT. (c) and (d), are the same as in (a) and (b), except for WNP.

17 Figure 4. (a) Cumulative seasonal (JASON) GPCP total rainfall amount (solid line),
18 AR(0) and total TC-rain amount (dot line), ARTC(0) from 1979 to 2005. (b)
19 Cumulative total TC frequency of occurrence (solid line) and TC accumulated rain
20 intensity (dot line), ARI, for NAT. Thick lines show 5-year running mean. (c) and
21 (d) are the same as in (a) and (b), except for WNP. Vertical dash lines separate the
22 pre-SSM/I and post-SSM/I period.

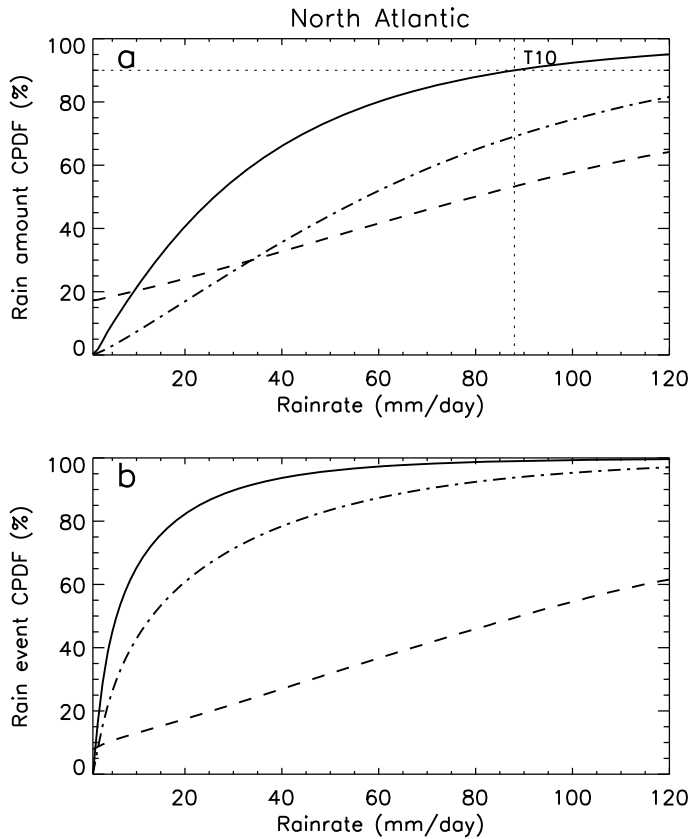
23 Figure 5. (a) Cumulative seasonal (JASON) GPCP rainfall amount (solid line), AR and
24 TC-rain (dot line), ARTC in T10 from 1979 to 2005. (b) Cumulative TC frequency

1 of occurrence (solid line) and TC average rain intensity (dot line) in T10 for NAT.
2 Thick lines show 5-year running mean. (c) and (d) are the same as in (a) and (b),
3 except for WNP. Vertical dash lines separate the pre-SSM/I and post-SSM/I period.

4 Figure 6. (a) Climatological frequency of occurrence (FOC) of SST binned with 0.5°C
5 interval, during JASON of the first 13 years (1979–1991, outlined bar) and the latter 13
6 years (1993–2005, filled bar), and (b) shift in FOC shown as the difference between the
7 SST FOC of the latter period (1993–2005) and the first period (1979–1991) normalized
8 by the mean of these two periods, for NAT. (c) and (d), as in (a) and (b), except for
9 WNP.

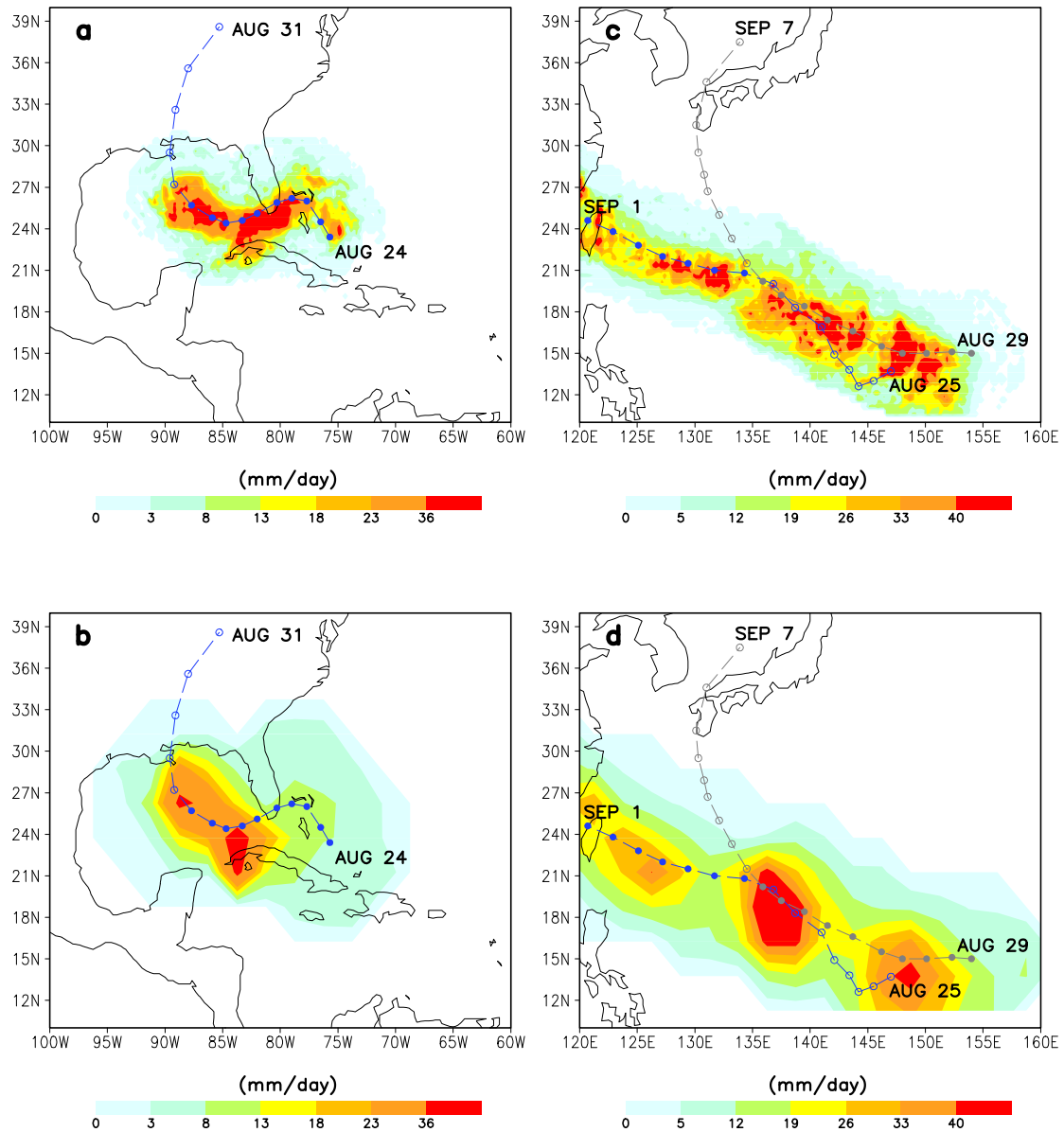
10 Figure 7. Time variation of ratio of cumulative extreme TC rainfall amount to total
11 rainfall, Ω , in T10 from GPCP (solid line). Dotted line shows the normalized
12 anomaly in percentage of warm pool area (defined as monthly SST>28°C) over
13 JASON season for each year for (a) NAT and (b) WNP. Thick lines show 5-year
14 running mean. Vertical dash lines separate the pre-SSM/I and post-SSM/I period.

15
16



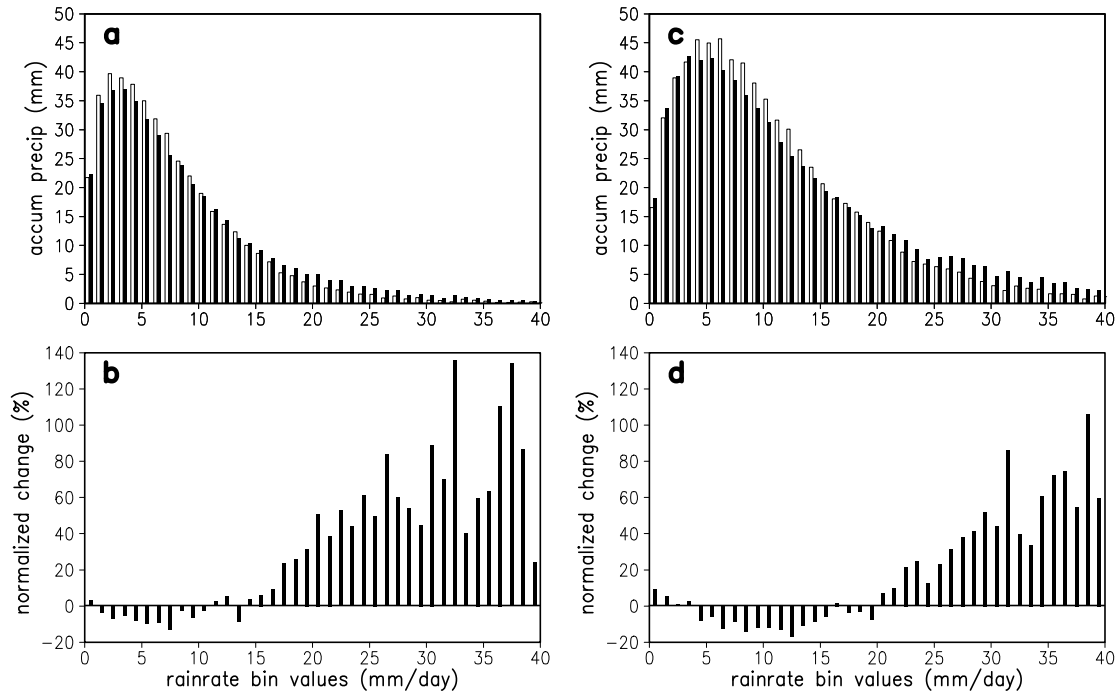
1

2 Figure 1. Cumulative PDF of daily rainfall (solid line), and TC-rain (dash-dot line) from
 3 TRMM data for NAT during JASON, 1998–2005, for (a) rainfall amount and (b) frequency
 4 of occurrence. The dashed line in (a) shows the fractional TC-rain to total rain amount, Ω ,
 5 and in (b) the fractional TC events to total rain events. The label T10 corresponds to CPDF =
 6 90% and threshold rain rate of approximately 88 mm/day.



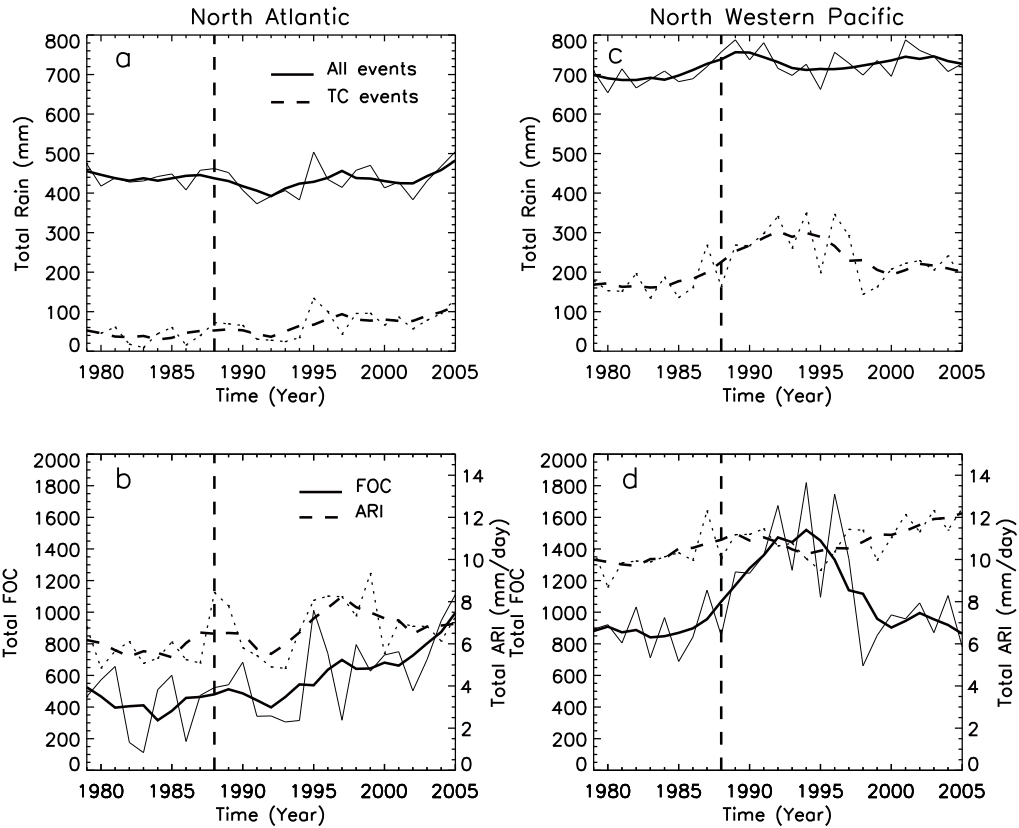
1
2
3
4
5
6
7

Figure 2. TC-rain from (a) TRMM and (b) GPCP during Aug 24–28, 2005 overlay with best track of Hurricane Katrina. TC-rain from (c) TRMM and (d) GPCP during Aug 29 – Sep 2, 2005 overlay with best tracks of Typhoons Nabi and Talim.



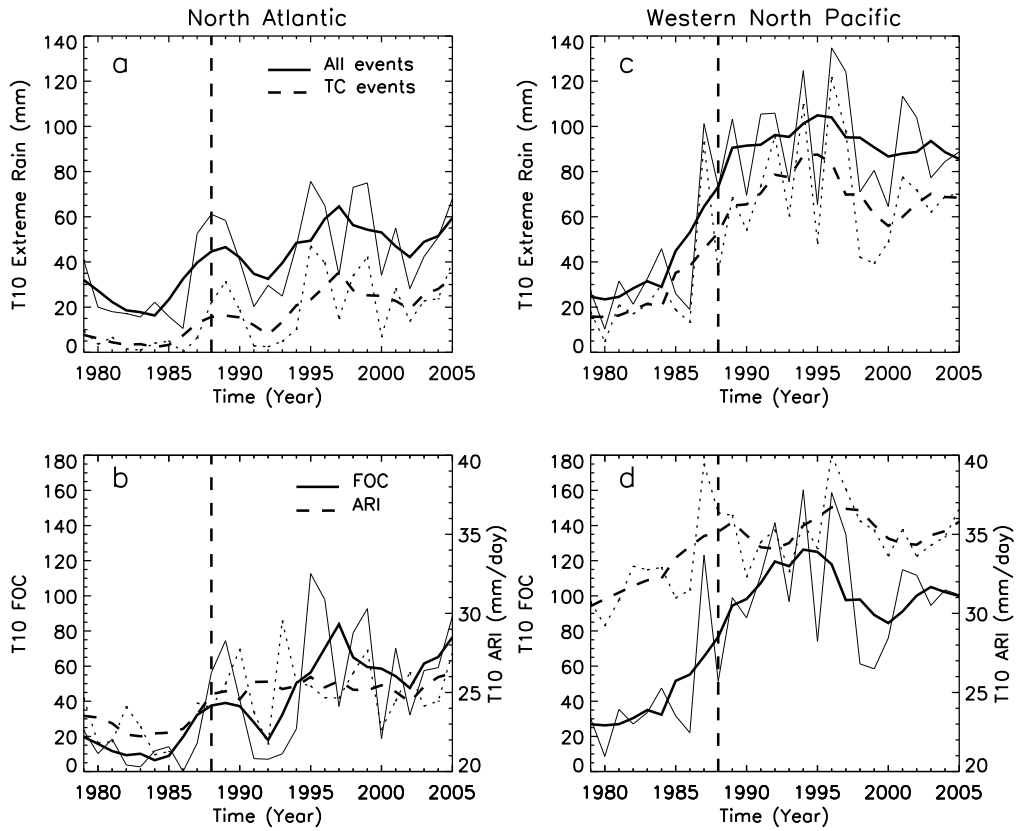
1

2 Figure 3. (a) The climatological PDF from GPCP for JASON accumulated rainfall
 3 amount at each rainfall bin (with 1 mm/day interval) of the first 13 years (1979–1991,
 4 outlined bar) and the latter 13 years (1993–2005, filled bar), and (b) shift in PDF shown
 5 as the difference between the rainfall PDF of the latter period (1993–2005) and the first
 6 period (1979–1991) normalized by the mean of these two periods for NAT. (c) and (d),
 7 are the same as in (a) and (b), except for WNP.



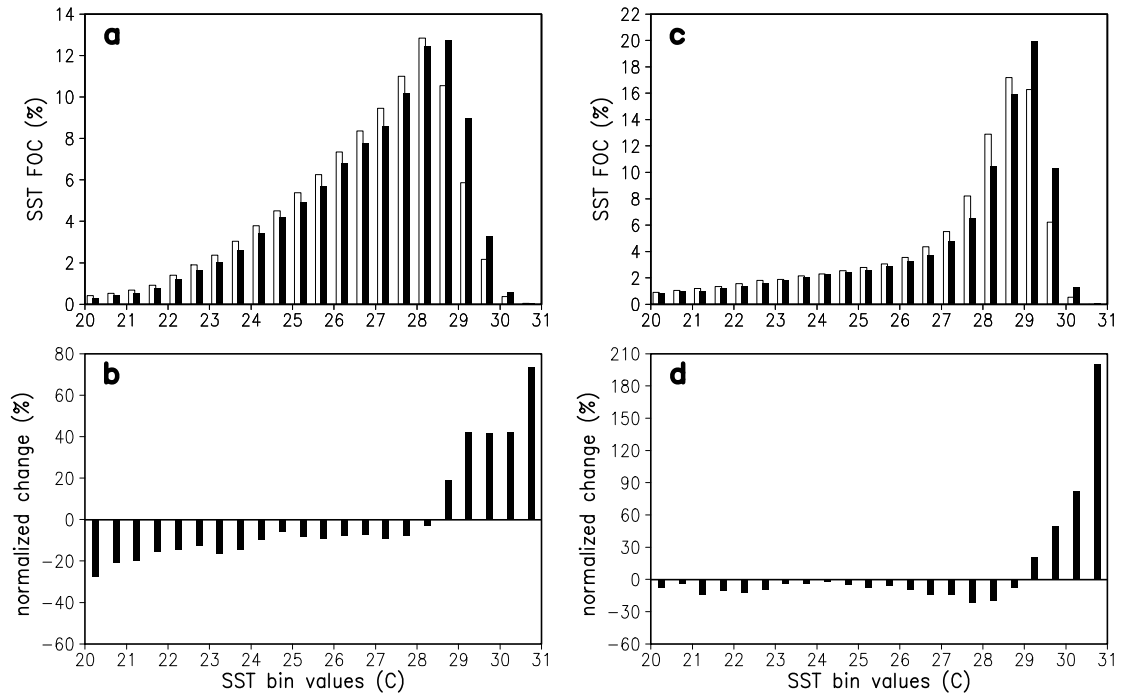
1
2 Figure 4. (a) Cumulative seasonal (JASON) GPCP total rainfall amount (solid line),
3 $AR(\mathbf{0})$ and total TC-rain amount (dot line), $AR_{TC}(\mathbf{0})$ from 1979 to 2005. (b) Cumulative
4 total TC frequency of occurrence (solid line) and TC accumulated rain intensity (dot
5 line), ARI , for NAT. Thick lines show 5-year running mean. (c) and (d) are the same as
6 in (a) and (b), except for WNP. Vertical dash lines separate the pre-SSM/I and post-
7 SSM/I periods.

8
9
10
11
12



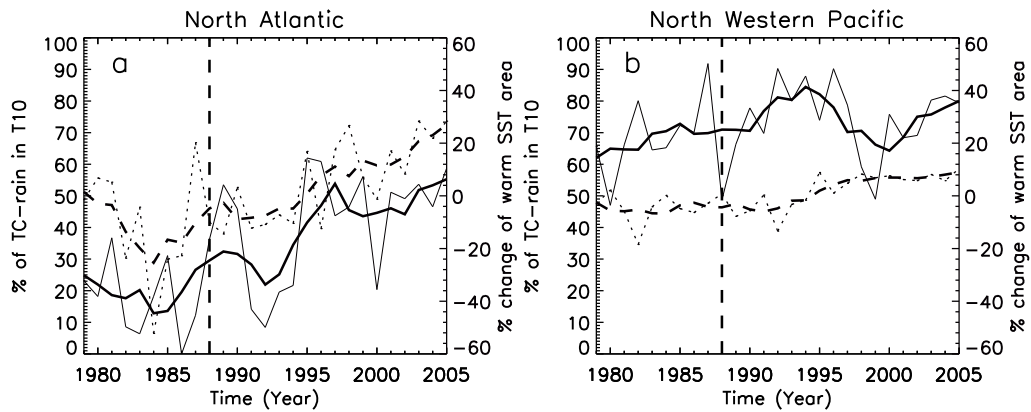
1
 2 Figure 5. (a) Cumulative seasonal (JASON) GPCP rainfall amount (solid line), AR and
 3 TC-related rainfall (dot line), AR_{TC} in T10 from 1979 to 2005. (b) Cumulative TC
 4 frequency of occurrence (solid line) and TC average rain intensity (dot line) ARI in T10
 5 for NAT. Thick lines show 5-year running mean. (c) and (d) are the same as in (a) and
 6 (b), except for WNP. Vertical dash lines separate the pre-SSM/I and post-SSM/I periods.

7
 8
 9
 10
 11



1
 2 Figure 6. (a) Climatological frequency of occurrence (FOC) of SST binned with 0.5°C
 3 interval, during JASON of the first 13 years (1979–1991, outlined bar) and the latter 13 years
 4 (1993–2005, filled bar), and (b) shift in FOC shown as the difference between the SST FOC
 5 of the latter period (1993–2005) and the first period (1979–1991) normalized by the mean of
 6 these two periods, for NAT. (c) and (d), as in (a) and (b), except for WNP.

7



1

2 Figure 7. Time variation of ratio of cumulative extreme TC rainfall amount to total
 3 rainfall, Ω , in T10 from GPCP (solid line). Dotted line shows the normalized anomaly in
 4 percentage of warm pool area (defined as monthly SST > 28°C) over JASON season for
 5 each year for (a) NAT and (b) WNP. Thick lines show 5-year running mean. Vertical
 6 dash lines separate the pre-SSM/I and post-SSM/I periods.

7

8